Articles

Remarkable Rate Enhancement of Orotidine 5′-Monophosphate Decarboxylase Is Due to Transition-State Stabilization Rather Than to Ground-State Destabilization†

Arieh Warshel,* Marek Štrajbl, Jordi Villà, and Jan Florián

Department of Chemistry, University of Southern California, Los Angeles, California 90089-1062

Received April 28, 2000; Revised Manuscript Received September 26, 2000

ABSTRACT: The remarkable rate enhancement of orotidine 5′-phosphate decarboxylase (ODCase) has been attributed to ground-state destabilization (GSD) by desolvation and more recently to GSD by electrostatic stress. Here we reiterate our previous arguments that the GSD mechanisms are not likely to play a major role in enzyme catalysis and analyze quantitatively the origin of the rate enhancement of ODCase. This analysis involves energy considerations and computer simulations. Our energy considerations show that (i) the previously proposed desolvation mechanism is based on an improper reference state; (ii) a nonpolar active site cannot account for the catalytic effect of the enzyme; (iii) the focus on the role of the negatively charged protein residues in the electrostatic stress GSD mechanism overlooks the fact that the positively charged Lys72 strongly stabilizes the substrate; (iv) although the previous calculation of the actual enzymatic reaction correctly reproduced the observed rate enhancement, it could not obtain this rate enhancement from the calculated binding energies (which are the relevant quantities for determining GSD effects); (v) the GSD mechanism is inconsistent with the observed binding energy of the phosphoribosyl part of the substrate; and (vi) the presumably unstable substrate (orotate) can be stabilized, at equilibrium, by accepting a proton from the solvent. Our computer simulation studies involve two set of calculations. First, we study the catalytic reaction by using an empirical valence bond potential surface calibrated by ab initio calculations of the reference solution reaction. This calculation reproduces the observed catalytic effect of the enzyme. Next, we use free-energy perturbation calculations and evaluated the electrostatic contributions to the binding energies of the ground state and transition state (TS). These calculations show that the rate enhancement in ODCase is due to the TS stabilization rather than to GSD. The differences between our own and the previous theoretical analyses stem from both the selection of the reacting system and the treatment of the long-range electrostatic contributions to the binding energy. The reacting system was previously assumed to encompass only the orotate. However, this selection does not allow proper description of the reaction catalyzed by the enzyme (i.e., [Orotate$^-$ + LysH$^+$] ⇔ [uracil + Lys + CO_2]). Therefore, the reacting system should include both orotate and the general acid in the form of the protonated Lys72 protein residue. This selection leads to a simple and consistent interpretation of the catalytic effect where the electrostatic stabilization of the transition state is due to the fact that the two negatively charged aspartic residues are already placed near the reactive lysine so that they do not have to reorganize significantly during the reaction. Interestingly, even calculations with only orotate$^-$ as the reacting system do not produce sufficient destabilization to account for a GSD mechanism. In summary, we conclude, in agreement with previous workers, that ODCase catalyzes its reaction by electrostatic effects. However, we show that these effects are associated with TS stabilization due to a reduction in the protein−protein reorganization energy and not with protein−substrate destabilization effects.

The idea that enzymes work by increasing their ground state (GS)[1] free energy has been frequently advanced (*1*−*3*). The most popular form of this proposal invokes nonpolar active sites, i.e., substrate destabilization by desolvation. Other alternatives for ground-state destabilization (GSD) may involve repulsive electrostatic interactions between the enzyme and the reacting region of the substrate. Decarboxylation reactions have been frequently considered as natural candidates for GSD by nonpolar environment (*4*, *5*).

A substrate destabilization mechanism has been suggested by several research groups (*5*−*8*) for the decarboxylation of orotidylic acid (OMP) to uridylic acid (UMP) by orotidine

† This work was supported by Grant GM24492 from the National Institutes of Health. J.V. wants to acknowledge EMBO fellowship ALTF 509-1998.

* To whom correspondence should be addressed.

[1] Abbreviations: EVB, empirical valence bond; ODCase, Orotidine 5′-phosphate decarboxylase; GSD, ground-state destabilization; HF, Hartree−Fock; LD, Langevin dipoles; LRA, linear response approximation; FEP, free-energy perturbation; PDLD, protein dipoles Langevin dipoles; LRF, local reaction field; SCAAS, surface constraint all atom solvent; P^{2-}, the phosphoribosyl moiety; [S^-], the orotate moiety; [LH^+], the protonated Lys72.

10.1021/bi000987h CCC: $19.00
Published on Web 11/08/2000

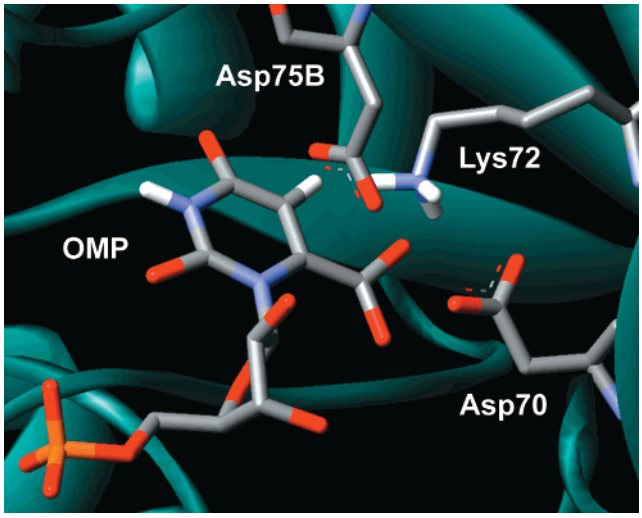

FIGURE 1: Active-site region of ODCase.

5′-phosphate decarboxylase (ODCase). This enzymatic reaction represents the final step in the de novo biosynthesis of pyrimidine nucleotides. The catalytic mechanism of ODCase attracted significant attention, in part due to the insightful analysis of Radzicka and Wolfenden that identified ODCase as the nature's most proficient enzyme (*9*). These authors found[2] that the activation barriers $\Delta g^{\ddagger}$ (that correspond to k_{cat}/K_M) and $\Delta g^{\ddagger}_{cat}$ (that correspond to k_{cat}) are 6.9 and 15.4 kcal/mol, respectively, while the activation barrier $\Delta g^{\ddagger}_{w}$ for the nonenzymatic reaction is 38.8 kcal/mol. The first theoretical attempt to explain the action of ODCase (*5*) concluded that the enzyme utilizes nonpolar or gas-phase-like hydrophobic environment to catalyze the decarboxylation reaction. This mechanism was criticized by Warshel and Florián (*10*) who pointed out that in any case of significant catalysis the substrate is surrounded by very polar rather than nonpolar environment. Recent crystallographic studies confirmed the presence of such polar (salt-like) environment (*7*, *8*, *11*) (see Figure 1). However, these structures were interpreted by Wu et al. (*8*) and Appleby et al. (*7*) as an evidence for reactants state destabilization by the interaction between the carboxylate group of the substrate and negative groups of the active site. According to their proposal, the very strong binding by the phosphoribosyl group pulls the remaining part of OMP (orotate) to its unfavorable environment, which leads to a large GSD effect.[3] Thus, the validity of the GSD mechanism in ODCase has been largely inferred from the identification of two Asp residues near the substrate and the reasonable possibility that these residues are negatively charged. However, this oversimplified analysis overlooked the fact that there is also a positively charged group (Lys72) in the vicinity of the substrate. To take into account all the contributions to GSD, the energetics of the ground-state substrate should be determined by very challenging calculations that must consider the proper ionization states of the protein and treat correctly long-range effects. The calculations of Wu et al. (*8*) made an important step in this direction, but they left major conceptual questions open and also have not provided an actual computational proof of the GSD mechanism (vide infra).

The present work exploits the structural information about ODCase to reexamine the origin of the rate enhancement of this remarkable enzyme. This is done by combining computational methods ranging from ab initio calculations of the reference solution reaction to empirical valence bond (EVB) simulations (*12*) of the reaction in the enzyme active site and in solution. We also used microscopic free-energy perturbation (FEP) calculations (*13*, *14*) and semimacroscopic protein dipoles Langevin dipoles (PDLD/S) (*15*) calculations in order to evaluate the electrostatic energies of the GS and transition state (TS) of the decarboxylation reaction. The calculations reproduce the observed trend with TS stabilization rather than the GSD mechanism.

Our study starts by demonstrating the general problems with the desolvation mechanism, focusing on a model that involves a hypothetical nonpolar enzyme. We then evaluate the catalytic effect of the actual enzyme using different computational strategies. These computations and an energy-based conceptual analysis provide several compelling reasons why the GSD mechanisms cannot work in ODCase and show that this enzyme utilizes electrostatic TS stabilization mechanism.

SIMULATION METHODS

To provide a reliable structure−function correlation and to analyze the origin of the catalytic effect of ODCase, it is essential to use sufficiently accurate computational models. As a first step in the analysis of the catalytic effect of the enzyme it is crucial to have a clear description of the corresponding reference reaction in solution (for the assumed reaction mechanism). The present work evaluates the free-energy surfaces of the solution reaction using an hybrid ab initio (*ai*)/Langevin dipole (LD) solvation model as implemented in the program ChemSol 2.0 (*16*, *17*). This *ai*/LD model has been found to give reliable potential surfaces for chemical reactions in solution (*18*, *19*). More specifically, we considered a model system that included NH_4^+ and orotate (Figure 2). The surface was mapped by series of partial ab initio HF/6-31G* geometry optimizations, in which the C6−C7 distance was varied from 1.5 Å (reactant state) to 4 Å (product state) and the proton was transferred from NH_4^+ to C6. To avoid structural artifacts caused by the unscreened electrostatic interactions between positively and negatively charged groups, some of the internal coordinates were kept frozen during these gas-phase geometry optimizations. Namely, the N···C6 distance was kept fixed at 2.8 Å (except for the reference point where this distance was set to 3.5 Å), the N···N1−C6 angle was set to 75°, and the torsional angle N···N1−C6−C7 was set to 64°. The gas-phase energies were determined by single point B3LYP/AUG-cc-pVDZ calculations. All ab initio calculations were

[2] Radzicka and Wolfenden (*9*) obtained $k_w = 2.8 \times 10^{-16}$ s^{-1}, $k_{cat} = 39$ s^{-1}, and $k_{cat}/K_M = 5.6 \times 10^7$s^{-1} M^{-1}. This gives $\Delta g^{\ddagger}_{w} = 38.8$ kcal/mol, $\Delta g^{\ddagger}_{cat} = 15.4$ kcal/mol, and $\Delta g^{\ddagger} = 6.9$ kcal/mol.

[3] Wu et al. (*8*) considered their GSD as a demonstration of Jencks' Circe effect (*2*, *44*). Jencks defined the Circe effect as "the utilization of strong attractive force to lure a substrate into a site in which it undergoes an extraordinary transformation" (which does not explain how the transformation is done). However, it is clear that his writing has involved the proposal that enzymes use binding energies to bring their substrate to unfavorable configurations where $\Delta g^{\ddagger}_{cat}$ is reduced by GSD (see the Appendix of ref *44*). Nothing is fundamentally wrong with Jencks' proposal from a thermodynamic point of view. However, this GSD might not be used by enzymes (as is repeatedly demonstrated by our works (see, e.g., ref *42*). Thus, the validity of the GSD has to be examined by free-energy calculations of the binding of the GS and TS in the protein and in water.

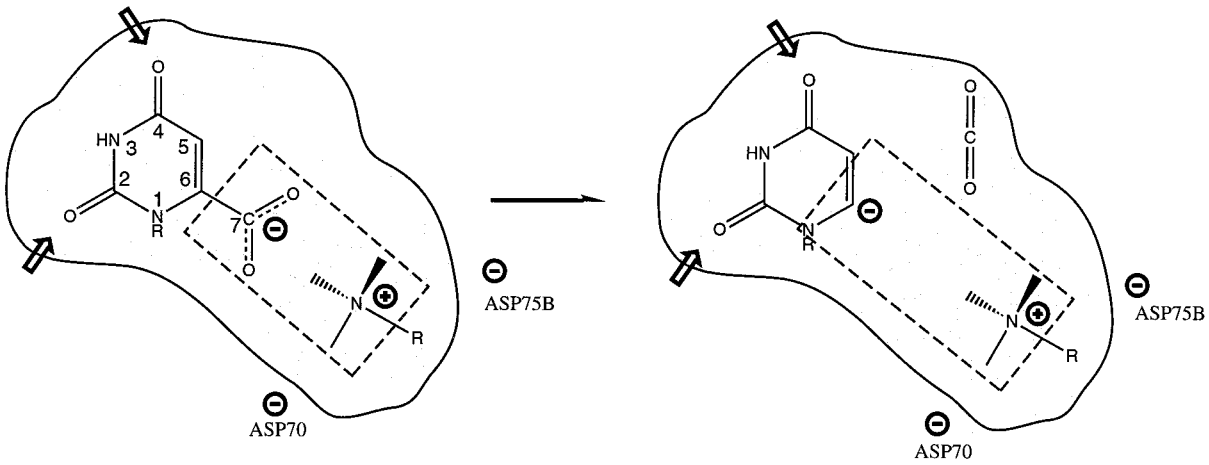

FIGURE 2: Schematic description of the reacting system considered in the present study. The figure depicts the rate determining step in the lysine-assisted mechanism assumed for ODCase. This figure includes in addition to the orotate + $LysH^+$ reaction system a schematic description of the protein environment (this environment is replaced with water in the *ai*/LD calculations). The figure also illustrates the fact that the mechanism involves a significant increase in the dipole moment of the reacting system upon transfer from the reactants state to the transition state.

carried out with the Gaussian 94 program (*20*). The proper polarization of the solute by the solvent was accomplished by using the polarized continuum model implemented in the Gaussian 94 program. A more detailed account of the *ai*/LD methodology used here can be found in ref *19*.

A model for the enzyme was constructed from the crystal structure of the 6-azauridine 5′-monophosphate (6-azaUMP) complex of the ODCase (PDB entry code 1DVJ) (*8*). After substituting the 6-azaUMP by the orotidine 5′-monophosphate, the complex was relaxed by 100 ps molecular dynamics (MD) simulation at 300 K with harmonic restrains of 0.06 kcal/(mol $Å^2$) on the positions of protein atoms to allow the protein structure to adjust in the presence of the new ligand. The energetics of the reaction in the enzyme could have been studied (in principle) by a hybrid quantum mechanical/molecular mechanics (QM/MM) approach (*21*−*25*). Such an approach is quite promising and has been used, with a semiempirical QM surface, in the study of Wu et al. (*8*). However, the implementation of the QM/MM approach with a high level ab initio surface for the QM region and proper free-energy calculations is still very challenging (*26*). Thus, we evaluated the free-energy surface of the reaction in the enzyme using the EVB method (*12*, *27*). The EVB has been used extensively for studies of reactions in enzymes and in solutions (e.g., refs *12*, *27*, and *28*), and at present, it is probably the most reliable way to study enzyme catalysis (i.e., the difference between the activation barrier in the enzyme and in the reference solution reaction). The EVB approach is described in detail elsewhere (*12*, *28*) and we will only note below a few points.

The EVB surfaces are obtained by representing the reacting fragments in terms of several valence bond-type configurations (resonance structures) and allowing the charges of these configurations to interact with their surrounding (enzyme and/or solvent) and then mixing the energies of these diabatic "solvated" configurations to obtain the adiabatic potential surface of the given reacting system. The EVB surfaces for the reaction in solution are parametrized here using the *ai*/LD surfaces of the given reference reaction and then using the same parameters to evaluate the potential surface for the reaction in the enzyme active site. The relevant activation free energies are evaluated by a combined free-energy perturbation (FEP)/umbrella sampling method (*29*). This approach maps the system from one resonance structure to another by a FEP procedure and uses umbrella sampling to evaluate the free energy of the actual ground-state surface obtained by mixing the different resonance structures. The FEP/umbrella sampling procedure allows us to evaluate nonequilibrium solvation effects which are neglected in other QM/MM studies (see ref *30*). Regular FEP was also used in an adiabatic charging procedure (*13*), in which the charges of the atoms in region I were changed from zero to their actual values. This calculation was done in both the reactant and the transition state, and in both the enzyme active site and solution. The calculated free-energy differences ($\Delta\Delta G_{sol}^{w\rightarrow p}$) were used to examine whether the given state is stabilized or destabilized by the protein.

Our simulations involved the local reaction field (LRF) treatment of long-range interactions (*31*), the polarizable model of the enzyme (*15*), and the surface constraint all atoms model (SCAAS) polarization constraints (*15*). The combination of the LRF and SCAAS methods is important for a proper microscopic treatment of long-range electrostatic effects, which is still not done properly in many simulations of charged groups in protein interiors. A proper treatment of long-range effects is particularly crucial in calculations that involve charge formation or anihilation (this will be needed in our binding calculations). Note in this respect that the study of Wu et al. (*8*) used a very approximated Born correction in an attempt to correct the use of cutoff in the calculation of long-range effects. The SCAAS/LRF treatment divides the system into several regions (see ref *15* for a detailed discussion), the inner being the reacting region (region I). This region is surrounded by a protein + solvent sphere (region II); a surface-constrained region where the average polarization and position of the solvent molecules is determined by special boundary conditions (region III); and a surrounding region (region IV) where the protein atoms are held with a strong constraint and where the electrostatic interaction between the protein + solvent and the internal region is replaced by the effect of a dielectric continuum with a dielectric constant $\epsilon_{bulk} = 80$. In the present calcula-

tions, two different settings for region I were employed. In the first calculation, only the orotate is included in region I, and in the second one we include also the N_ζ of Lys64 with its bonded hydrogen atoms.

The FEP calculations in both the EVB free-energy profile evaluation and in the adiabatic charging were carried out after 100 ps equilibriation time using 11 frames and a 30 ps simulation time for each frame, with 1 fs integration time step. The radius for region II as well as the radius for the water sphere were set to 16.0 Å, and the radius for the Langevin dipoles sphere was set to 18.0 Å in the FEP evaluation of the free-energy profile. These radii were set to 18.0, 18.0, and 20.0 Å, respectively, for the adiabatic charging FEP calculation. All the MD, FEP, and EVB/FEP calculations were performed using the program ENZYMIX (*15*).

It might be important to point out to those who are not familiar with the EVB approach that our calculations (with a proper ab initio calibration) are likely to be more quantitative than the semiempirical hybrid quantum mechanical/molecular mechanics (QM/MM) calculations of Wu et al. (*8*). That is, the QM/MM calculations used semiempirical model whose energy was calibrated to reproduce the observed energy in solution, but the semiempirical charge distribution was not calibrated. On the other hand the EVB method starts with high level ab initio charge distribution and provides a consistent way for reproducing the change of these charges in the given environment.

In addition to the microscopic EVB simulations, we used the semimicroscopic version of the protein-dipoles Langevin-dipoles model (PDLD/S) (*15*) in its linear response approximation (LRA) implementation. The PDLD/S-LRA calculations were carried out to evaluate the relevant electrostatic energies. The LRA averages were done over five protein configurations for the polar (or charged) and nonpolar states of each state studied. These configurations were generated by 1 ps unconstrained MD simulations of the enzyme−substrate complex. The radius of the water sphere in the PDLD/S calculation was set to 16.0 Å. Further details of the PDLD/S-LRA approach are described elsewhere (*15*, *32*). The PDLD/S-LRA was also used in calculating the pK_as of the protein residues using the protocol described in ref. (*32*). These PDLD/S calculations involved the use of a "protein dielectric", ϵ_p, that plays an important role in the determination of the intrinsic pK_as and an effective dielectric constant, ϵ_{eff}, for charge−charge interactions. The meaning of ϵ_p and ϵ_{eff} and their justification is explained and verified elsewhere (e.g., *12*, *32*, and *33*) and will not be rediscussed here. All the PDLD/S-LRA calculations were performed with the program POLARIS (*15*). Both the ENZYMIX and POLARIS programs have been recently integrated in the package MOLARIS (*34*).

REACTION IN A HYPOTHETICAL NONPOLAR ACTIVE SITE

As stated in the introductory portion of this paper, it is tempting to explain the large catalytic power of ODCase by involving the desolvation hypothesis. Indeed Lee and Houk (*5*) supported this hypothesis by a computational study that considered polar and nonpolar protein active sites. More specifically, they analyzed the transformation of the $LysH^+\cdots S^-$ ion pair (where S^- designates the orotate moiety) to a neutral transition state (Figure 3) using a quantum

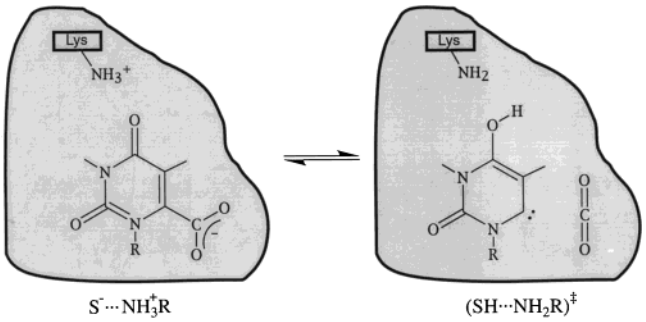

FIGURE 3: Reactant state ($S^-\cdots NH_3^+R$) and the transition state ($SH\cdots NH_2R)^‡$ proposed by Lee and Houk for the enzymatic decarboxylation of OMP (*5*). The $-NH_3^+$ and $-NH_2$ groups denote the catalytic lysine residue in the hypothetical nonpolar active site of ODCase.

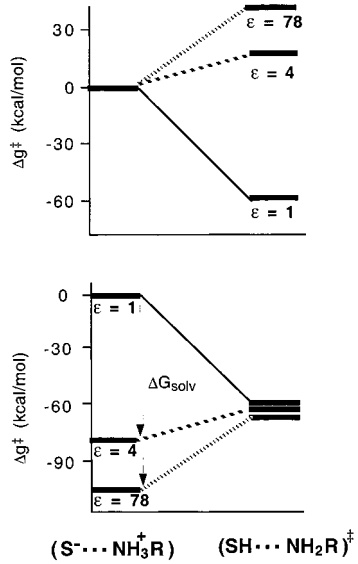

FIGURE 4: Energetics of the catalytic reaction of Figure 3 in an active site of a uniform dielectric constant. (Top) The results obtained by Lee and Houk (*5*) treated inconsistently (as was done in Table 1 of ref *5*) with the same energy assigned to the initial state in three different environments ($\epsilon \approx 1$, $\epsilon \approx 4$, and $\epsilon \approx 80$). Bottom: The correct plot of the results of Lee and Houk (*5*). Note that the solvation free energy (ΔG_{solv}) is added to the gas-phase energy of the $R-NH3^+\cdots S^-$ reference point.

mechanical continuum dielectric model. Their calculations indicated that the activation barrier for the reaction in a uniform medium of the dielectric constant $\epsilon = 4$ is about half of that in the polar environment with $\epsilon = 80$ (*5*). These results (which give the correct trend for the assumed model) were interpreted as an evidence that the extreme efficiency of ODCase can be attributed to its hypothetical nonpolar active site and that a nonpolar enzyme environment offers a general mechanism for enzyme catalysis. Here we point out the general problems associated with the idea of catalysis by nonpolar enzyme sites (see also refs *10* and *35*) and illustrate these concepts for the particular case of ODCase.

To understand the energetics of ODCase, it is important to use well-defined thermodynamic concepts, which include the effects of solvation energies and a single reference state. As illustrated in the upper part of Figure 4, considering the reaction *without* using a single reference state may lead us to the conclusion that in the nonpolar active site ($\epsilon = 4$) the activation barrier is lower than in a polar environment ($\epsilon = 80$).[4] However, when a single reference state (for example

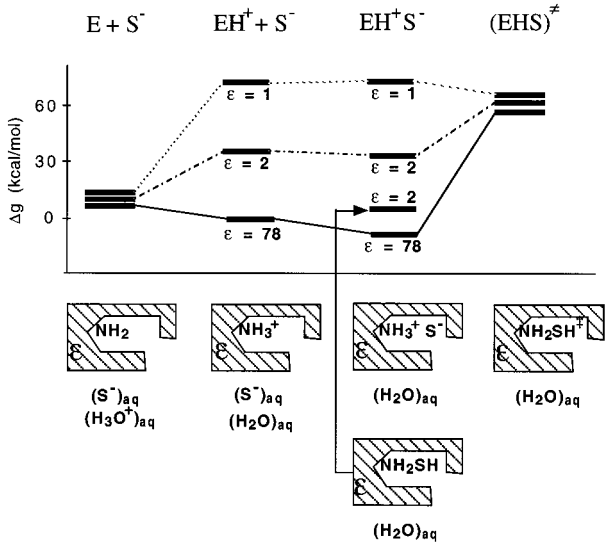

FIGURE 5: Schematic representation of the energetics for the Lee and Houk mechanism (Figure 3) of the decarboxylation reaction in a nonpolar ($\epsilon = 1$ and 2) and polar ($\epsilon = 80$) enzyme active sites. Note that the free energies of the reactants state ($S^-\cdots NH_3^+R$) in each environment involve the contribution of the corresponding solvation free energies. [The magnitude of this contribution was determined by the polarized continuum model (PCM HF/6-31G*) implemented in the Gaussian 94 program (*20*). The default Pauling's atomic van der Waals radii scaled by 1.2 were used. The calculated solvation free energies for orotate, $CH_3NH_3^+$, carbene$\cdots$methylamine complex, and CO_2 were -68, -76, -13.8, and -1.3 kcal/mol, respectively. For the ($S^-\cdots NH_3^+R$) state, in which the orotate and $CH_3NH_3^+$ ions were assumed to lie 6 Å apart, solvation free energy was estimated by using the generalized Born formula, where the gas-phase interaction energy of -55 kcal/mol was assumed. In addition, experimental binding free energy of the ODC$\cdots$OMP complex of -9 kcal/mol was taken into account.] As is clear from the figure, the reactants state energies are very different at different ϵ values (in contrast to the free-energy diagram presented in the upper part of Figure 4). Now the transition-state energy is nearly identical in different environments, and the experimental value of k_{cat} of 16 kcal/mol is obtained where ϵ is as low as 1.5.

the noninteracting enzyme and substrate in the gas-phase environment) is used the uncharged transition state has approximately the same energy in the three environments and the least stable ground state is the gas-phase ion pair (Figure 4, bottom).

To further clarify the problems with the desolvation mechanism we have to use a more quantitative energy considerations. This is done in Figure 5 for a hypothetical enzyme with a uniform polarity taking as general reference state the noninteracting enzyme and substrate molecules in aqueous solution ($E + S^-$). The figure considers relevant protonation states of the substrate and the enzyme. Here the highest activation barrier is involved in forming the $R-NH_3^+ + S^-$ ion pair in a vacuum-like environment. The problem remains but to a lesser extent in the $\epsilon = 2$ case. In this respect, it is important to realize that ion pairs are less stable in a nonpolar environment than in a polar environment (*36*). In other words, if one would try to catalyze reactions by a nonpolar enzyme site he would have to pay for bringing the charged substrate into the active site and consequently the overall $\Delta g^{\ddagger}$ (that corresponds to k_{cat}/K_M) would not be reduced.

A seemingly reasonable suggestion for overcoming the above-mentioned problem could invoke the fact that OMP contains a phosphate group, which can be stabilized by a polar site of the enzyme while still leaving the orotate in a low dielectric region. Thus, the unfavorable binding contribution from the nonpolar part of the enzyme cavity could be possibly overcome by the strong binding of the distant phosphate moiety. This is, in fact, a variant of Jencks' idea of using binding energy for GSD that has been invoked by Wu et al. (*8*). However, a more quantitative analysis should consider the overall reduction of the activation barrier upon going from aqueous solution to the enzyme active site and evaluate the difference between the activation barrier in water ($\Delta g_w^{\ddagger}$) and the activation barrier in the enzyme active site ($\Delta g_{cat}^{\ddagger}$). If the observed difference $\Delta g_w^{\ddagger} - \Delta g_{cat}^{\ddagger} \approx 23$ kcal/mol [1] was due to the reactants state destabilization then the overall observed binding free energy of -9 kcal/mol would require -32 kcal/mol binding free energy at the phosphate site. Such an enormous binding energy is without precedent. More importantly, we have now direct estimates of the phosphate binding energy (*11*) which are in the range of -15 kcal/mol rather than -30 kcal/mol. This point will be analyzed in more detail in the last section.

Another fundamental problem with the desolvation model (or related substrate destabilization models) is the fact that in the assumed nonpolar active site the lysine proton will be transferred to the carboxylate group, i.e., the EH^+S^- reactants state for the enzyme$-$substrate complex will not exist in $\epsilon = 4$. In other words, any large destabilization of the EH^+S^-reactants state in a nonpolar cavity will push the energy of this state above the energy of the neutral ESH complex (Figure 5), and thus the neutral state will constitute a new reactants state for the enzymic reaction.

Before leaving this section, it is important to clarify why the kinetics of solution reactions, which are frequently brought as chemical evidences for the desolvation hypothesis, are not so relevant to enzyme catalysis. That is, many chemical reactions (e.g., most S_N2 reactions) are accelerated in nonpolar solvents relative to the corresponding reaction in polar solvent. The reason is that the ground-state (GS) charge distribution is more localized and better solvated than the delocalized charges in the TS. Now the larger solvation of the GS is more pronounced in polars solvents (thus, the activation barrier is higher in polar solvents). This interesting phenomenon has led many chemists to embrace the desolvation hypothesis. However, as shown in Figure 6, this type of conjunction neglects one crucial aspect—namely that the energy of moving the reactants state from the polar to nonpolar solvent is invested by an *external* source. Therefore (if the difference between the reaction rate measured in nonpolar and polar solvents should be of any relevance to enzymatic reactions), the activation barrier measured in a test tube with a nonpolar solvent ($\Delta g_{np}^{\ddagger}$) should be augmented by the free energy of moving the substrate from water to non polar solvent ($\Delta G_{w\rightarrow np}$). Analogously, $\Delta g^{\ddagger}$ for an

[4] It is important to point out that due to the improper choice of the reactant reference state with no interaction between cation and anion, and due to the underestimated solvation free-energy difference between reactants and the transition state, $\Delta g_{cat}^{\ddagger}$ of LH in the $\epsilon = 4$ environment is largely underestimated (see captions of Figure 5). Consequently, to reach the observed catalytic effect with a more realistic continuum model, the dielectric constant of the protein active site must be smaller than 2. Such a small dielectric constant is typical for nonpolar solvents such as *n*-hexane or 1-pentene (*45*) but it is hardly attainable in any protein interiors.

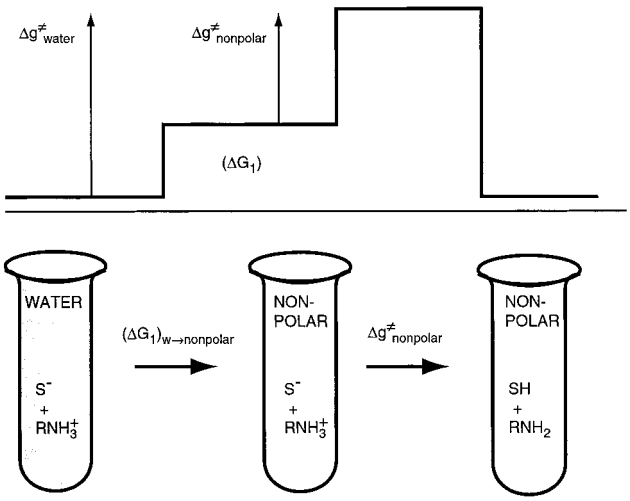

FIGURE 6: Schematic illustration of the problem with the assumption that the rate acceleration by nonpolar solvents is relevant to enzyme catalysis. As illustrated in this figure, a reaction in a test tube with a nonpolar solvent might be accelerated significantly, i.e., $\Delta g^{\ddagger}_{nonpolar} < \Delta g^{\ddagger}_{water}$. However, to *use* this information for enzymatic reactions, we need to consider the free energy associated with the transfer of the reactant from water to nonpolar solvents, $\Delta G_{w\rightarrow nonpolar}$. This contribution corresponds to the transfer of a substrate from water to a nonpolar enzyme.

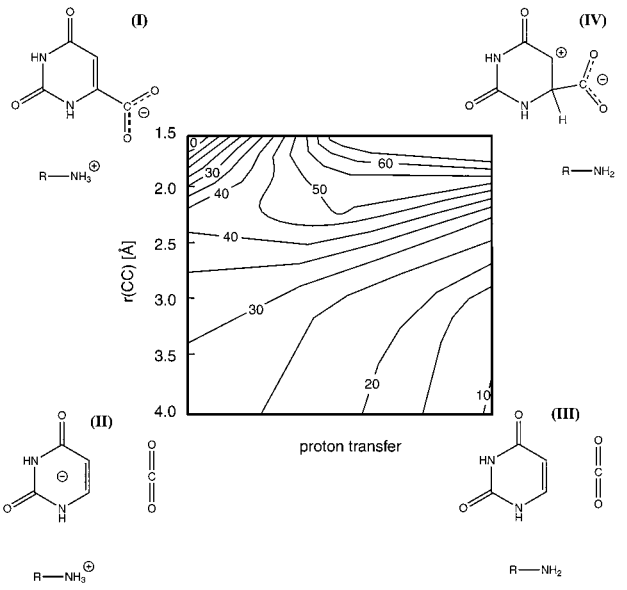

FIGURE 7: Calculated ai/LD potential surface for the decarboxylation reaction in aqueous solution. The potential is given in kilocalories per mol. r(CC) designates the C_6-C_7 distance (Figure 2) in angstroms and "proton transfer" corresponds to the extent of proton transfer from Lys72 to C_6 of the substrate.

enzymatic reaction includes the substrate binding energy, ΔG_{bind}, which reflects the energy of moving the substrate from water to the active site.

ENERGETICS OF THE REACTION IN THE ACTUAL ACTIVE SITE OF ODCASE

The availability of the three-dimensional structure of ODCase should allow one, at least in principle, to determine the energetics of the reaction catalyzed by this proficient enzyme. In converting the structural information to energetics, one should note first that the active site does not resemble at all the nonpolar environment needed for the desolvation mechanism and it is in fact very polar. This active site appears to have more negatively charged groups than positively charged groups near the carboxylate of the orotidine. This observation has been considered as a source for GSD effect (note, however, that the stabilizing effect of Lys72 was overlooked). Indeed, the calculations of Wu et al. (*8*) were interpreted as a proof of a GSD effect, in which the strong binding of the phosphate group presumably pulls the carboxylate to a region where it is repelled by the surrounding charges. The structure of ODCase with 6-aza-uridine-5′-monophosphate provides a strong indication that the decarboxylation reaction corresponds to the lysine-assisted mechanism. Indeed the energy profile obtained by Wu et al. (*8*) for this mechanism appears to nicely reproduce the observed magnitude of $\Delta g^{\ddagger}_{w} - \Delta g^{\ddagger}_{cat}$. However, the calculated profile cannot tell us whether the catalytic effect of the enzyme is due to GSD or TS stabilization. This issue was explored by Wu et al. by calculating the electrostatic component of the binding energy of the reacting part of the substrate in its ground and transition state. These calculations gave approximately equal destabilization for the ground and transition state of the reacting part of the substrate (Table 2 of ref *8*). This means that binding calculations underestimated the observed $\Delta g^{\ddagger}_{w} - \Delta g^{\ddagger}_{cat}$ by 21 kcal/mol. Nevertheless, the overall calculations were accepted as an evidence for the GSD mechanism.

To determine the origin of the catalytic power of ODCase, we carried out EVB/FEP calculations of the reaction profile, and FEP calculations of the binding energies of GS and TS. We started our study by calibrating the EVB surface for the lysine-assisted mechanism using an *ai*/LD calculation of the corresponding reference reaction in solution. The calculations modeled the $LysH^+$ group by NH_4^+. The calculated surface (Figure 7) has a least-energy path that corresponds to a stepwise mechanism with an initial cleavage of the C7−C6 bond followed by a proton transfer from $LysH^+$ to C6. The corresponding $\Delta g^{\ddagger}$ is about 40 kcal/mol. Interestingly, we were able to find a flat transition-state region where the carboxylate moves out of plane before the proton-transfer step. This region was explored in a preliminary way with HF rather than NH_4^+ as a general acid, including the correction for the pK_a difference (*19*) between HF and NH_4^+. These calculations, which are expected to be more reliable since they do not involve an ion-pair system, produced an activation barrier of about 35 kcal/mol. The calculated barrier is not directly related to the barrier of ∼38 kcal/mol measured by Radzicka and Wolfenden for the decarboxylation of methyl orotate in water (*9*). However, since the presence of 1 M methylamine-HCl buffer was found to have no effect on the rate for the decarboxylation in water (*9*), we have a lower limit of 38 kcal/mol for $\Delta g^{\ddagger}$ for the NH_4^+ assisted catalysis in water. Because our reference solution reaction should consider reactants in the common solvent cage where the general acid is at 55 M concentration (*12*), we obtain $\Delta g^{\ddagger}_{cage}(NH_4^+) \geq \Delta g^{\ddagger}_{w} - 2 = 36$ kcal/mol. Thus, we estimate $\Delta g^{\ddagger}_{cage}$ to be $\sim 38 \pm 4$ kcal/mol. Of course, there is nothing wrong in comparing the $\Delta g^{\ddagger}_{cat}$ to the observed $\Delta g^{\ddagger}_{w}$ obtained without the NH_4^+ general base. However, in this case we are not comparing the same reactions and the catalytic effect (if any) obtained by changing the chemistry would be rather trivial (it simply reflects the change of the reacting system).

Table 1: Calculated Activation and Reaction Free Energies of the Catalytic Reaction of ODCase[a]

	$\Delta g^{\ddagger}(\Delta G_{I\rightarrow II})$				
region I configuration	water	A	B	C	D
$[S^{-}LH^{+}] \rightarrow [S^{-}LH^{+}]^{\ddagger}$	38 (31)	24 (16)	22 (15)	17 (1)	19 (9)
$[S^{-}] \rightarrow [S^{-}]^{\ddagger}$	38 (26)	18 (0)	19 (3)	17 (−1)	23 (7)

[a] Activation and reaction free energies (kcal/mol) of the decarboxylation reaction in water and for different charge states of the protein ionizable groups. The reaction free energies of the first step of the reaction (the I → II step of Figure 7) are given in brackets. The part of the reacting system that is taken as region I is enclosed in square brackets. S and L designate the reactive part of the substrate (orotate) and Lys72, respectively. $[S^{-}]$ and $[S^{-}]^{\ddagger}$ designate, respectively, the reactive part of the substrate in its GS and TS structures and charge distributions. The calculations were performed by the FEP/umbrella sampling EVB approach. The dependence of the calculated results on the ionizations states of the protein residues is examined in columns A, B, C, and D, which correspond to calculations with the following ionized residues: (A) Asp75B, Asp70, Lys72, OMP phosphate; (B) Asp75B, Asp70, Lys72, Arg203, OMP phosphate; (C) set B plus Asp20, His98, His128, Lys82B; and (D) set B plus Asp20, Lys42, Glu25, Lys82B, Glu78B.

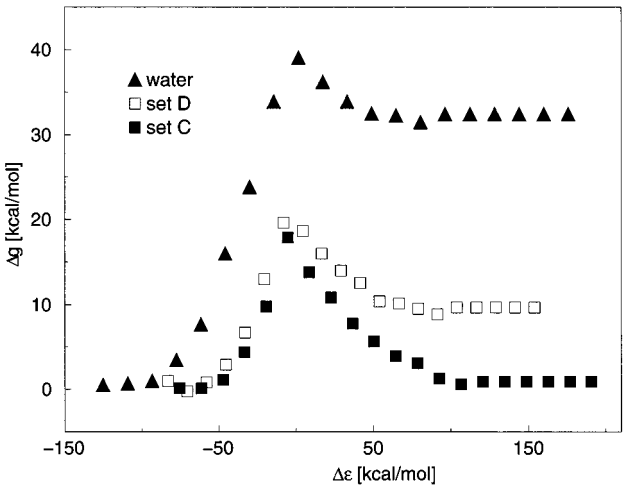

FIGURE 8: EVB free-energy surface for the decarboxylation reaction in ODCase and in a reference solvent cage. The figure presents the results of the simulations for two assumed ionization states of the protein (conditions C and D are the same as in Table 1). The calculations involve $[S^{-}LH^{+}]$ in region I.

Obviously, the validity of the GSD mechanism must be addressed using the same reactants in the enzyme and in solution. Thus, although the EVB surface was calibrated to reproduce $\Delta g^{\ddagger}_{cage} = 38$ kcal/mol, we keep in mind the realistic possibility that the lysine-assisted reaction in aqueous solution might have a somewhat lower barrier than that of the reaction without a general acid.

Before turning to the EVB calculation in the enzyme, it is crucial to have a clear idea about the ionization states of the protein residues. This is important since we are dealing with a highly charged system in a very heterogeneous environment and the results can depend strongly on the assumed ionization state of the protein. To determine the ionization state, we performed PDLD/S-LRA calculations, in which we considered the results for different limiting values of the protein "dielectric constants" ϵ_p and ϵ_{eff}, with ϵ_p in the range of 4−8, and ϵ_{eff} between 20 and 40 (the meaning of these parameters has been discussed extensively in our work; see e.g. ref *32*). It was found that Asp20, Asp70, Glu125, and Glu78B are ionized (negatively charged) at pH 7. Similarly, Lys42, Lys72, Lys 82B, Arg160, and Arg203 are ionized (protonated). Interestingly, the pK_a of Lys72 was found to be quite elevated and reached a value between 16 and 18. The ionization state of His98 and His128 is less certain, since it was found that His98 has a low pK_a between 1 and 4 while the calculated pK_a of His128 has a wide range, between 3 and 9. The ionization state of residues that lie farther than 12 Å from the substrate is less relevant since they are unlikely to affect the catalysis in a major way (the indirect structural effects of these residues are included in our calculations since we constrain the distant part of the protein to stay near its X-ray structure). The most likely ionization state was used in defining one of our simulation conditions (set D in Table 1). In addition, to examine the effect of different ionization states on the catalytic power of the enzyme, we considered three other ionization states (sets A, B, and C in Table 1).

After determining the protein ionization state and evaluating the *ai*/LD surface in water, we turn to the calibration of the EVB surface in aqueous solution. This was done by adjusting three diabatic energy surfaces ϵ_I, ϵ_{II}, and ϵ_{III} that correspond to the structures I, II, and III in Figure 7. The calibrated EVB surface was then used for the determination of the free-energy profile in water and in the protein active site. This was done by the FEP/umbrella sampling procedure, where the system was mapped gradualy by a FEP procedure from $\epsilon_I \rightarrow \epsilon_{II}$ and the corresponding free energies of the actual adiabatic ground-state surface (obtained by mixing the three resonance structures) were determined by an umbrella sampling procedure (see, for example, ref *29*). The surface was not mapped along the II → III step, since the least-energy path corresponded to a stepwise rather than a concerted mechanism, and the II → III proton-transfer step is not rate determining. Note that the EVB calculations force the system to sample configurations at the transition-state region without the need to constrain the system to a specific structure. The simulation conditions are described in the methods section and the corresponding results are summarized in Table 1 and Figure 8.

Table 1 presents the activation free energies, $\Delta g^{\ddagger}_{cage}$, obtained by the EVB/FEP calculations for the reaction in water and in the active site for two different region I constituents and four different ionization states of the surrounding protein. When $[S^{-}LH^{+}]$ was included in region I (here we designate Lys72 by L), we obtained $\Delta g^{\ddagger}_{cat}$ between 17 and 24 kcal/mol. We also obtained $\Delta g^{\ddagger}_{cat}$ between 17 and 23 kcal/mol when only $[S^{-}]$ was in region I. The free-energy profile for the reaction in water and in the enzyme active site for sets C and D with $[S^{-}LH^{+}]$ in region I is given in Figure 8. As seen from Table 1 and the figure, we obtained a reduction of activation barrier between 21 and 15 kcal/mol for the most realistic ionization states of the protein (sets C and D) in our model, in a reasonable agreement with the observed reduction of ∼23 kcal/mol (see footnote 2). As will be argued below our final conclusions will be independent of the exact reproduction of $\Delta g^{\ddagger}_{cage} - \Delta g^{\ddagger}_{cat}$. Also note that the $\Delta g^{\ddagger}_{w} - \Delta g^{\ddagger}_{cat}$ of 22.4 kcal/mol was obtained by Wu et al. using different computational methods for the calculation of $\Delta g^{\ddagger}_{w}$ and for the calculations of $\Delta g^{\ddagger}_{cat}$. Furthermore, these authors have not examined the sensitivity of the calculated $\Delta g^{\ddagger}_{cat}$ to

Table 2: Calculated Binding Free Energies of Different States and Configurations Which Are Involved in the Catalytic Reaction of ODCase[a]

	$\Delta\Delta G_{sol}^{w\rightarrow p}$			
configuration	A	B	C	D
$[S^-]$	1	−9	4	−3
$[S^-]^‡$	−11	−17	−21	−23
$[S^-LH^+]$	−20	−27	−28	−30
$[S^-LH^+]^‡$	−55	−50	−58	−47

[a] Electrostatic contributions to the binding free energies (in kcal/mol) of the indicated configurations of region I. The corresponding contributions ($\Delta\Delta G_{sol}^{w\rightarrow p}$) were evaluated by FEP calculations that involve changing the charge of atoms in region I from zero to their actual value in the given configuration. A, B, C, and D refer to different charge configurations of the active site (see captions of Table 1).

the protein ionization states, and their $\Delta g_w^‡ - \Delta g_{cat}^‡$ became only 2 kcal/mol when it was evaluated from the calculated binding energies of GS and TS. These points are not intended as a criticism of Wu et al. instructive study, but rather as a reminder for the reader that FEP calculations do not automatically give perfect results for highly charged groups in protein interiors and that the use of binding energy in assessing catalytic effects is very challenging.

The reproduction of the catalytic effect does not tell us, however, whether this effect is due to TS stabilization or GSD. To resolve this crucial issue, it is essential to evaluate separately the binding energy of the GS and TS. Thus, we calculated the change in the solvation free energy, $\Delta\Delta G_{sol}^{w\rightarrow p}$, upon moving region I in its ground or transition state from water to the active site of ODCase. Table 2 gives the $\Delta\Delta G_{sol}^{w\rightarrow p}$ obtained by FEP calculations for the case where only $[S^-]$ is in region I and for the case where $[S^-LH^+]$ is in region I. Although the results depend on the simulation conditions, we obtain in all cases significant catalysis (similar to that obtained with the direct calculations in Table 1). More importantly, we obtained a very large GS stabilization for $[S^-LH^+]$, and even for $[S^-]$ we did not obtain a large GSD. Apparently, our results are different than those of Wu et al., who obtained $\Delta\Delta G_{sol}^{w\rightarrow p}$ of ∼18 kcal/mol for $[S^-]$. However, as stated above, Wu et al. also obtained $\Delta\Delta G_{sol}^{w\rightarrow p}$ of ∼16 kcal/mol for $[S^-]^‡$ and, thus, have not reproduced the catalytic effect of the enzyme. The PDLD/S-LRA calculations with $\epsilon_p = 4$ and $\epsilon_{eff} = 40$ gave $\Delta\Delta G_{sol}^{w\rightarrow p}$ of 10, 11, 3, and 6 kcal/mol for sets A, B, C, and D, respectively, when $[S^-]$ was included in region I and −36, −38, −29, and −28 kcal/mol for sets A, B, C, and D when $[S^-LH^+]$ was included in region I.

As established by our calculation, the binding energy of $[S^-]$ is close to zero and not very positive (−3 to 6 for sets C and D), while the binding energy of $[S^-LH^+]$ is clearly very negative. The significance of these findings will be discussed in the next section.

THE CATALYTIC EFFECT OF ODCASE IS DUE TO TS STABILIZATION

Before examining the actual origin of the catalytic effect of ODCase, it is useful to point out fundamental problems with the proposal that the catalytic effect is due to GSD of the orotate moiety. First, a major destabilization of the negatively charged orotate by either nonpolar environment

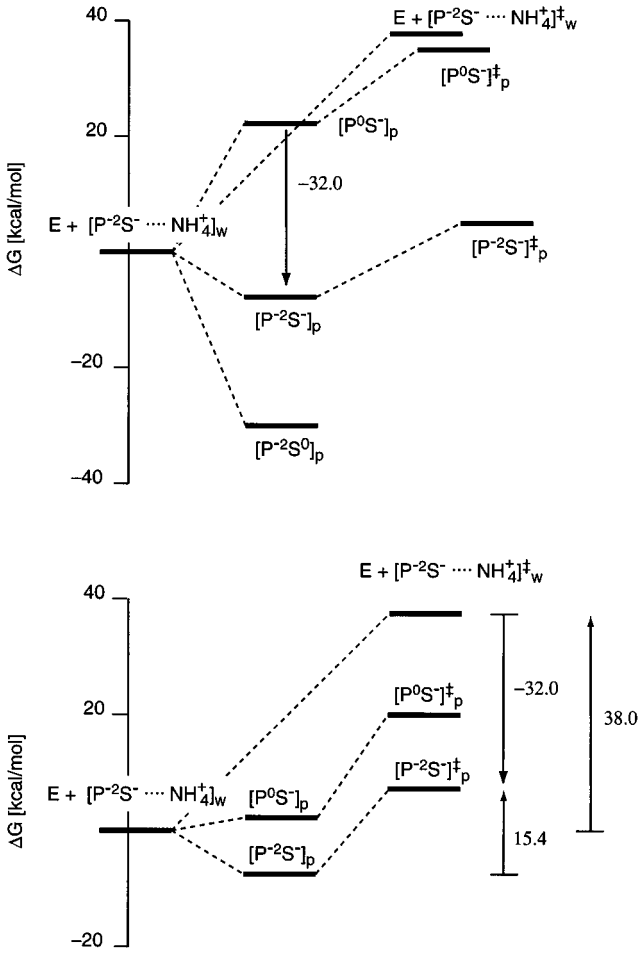

FIGURE 9: Overall energetics of the reaction of ODCase in the GSD (top) and the TS (bottom) stabilization mechanisms. P^{2-} indicates the phosphoribosyl residue.

or negatively charged environment will lead at equilibrium to a new reactants state where the substrate or a negatively charged protein residues are protonated (see below). Second, an enormous binding free energy of about −32 kcal/mol is needed for the GSD mechanism (such a strong binding is needed to compensate for the assumed large destabilization of the orotate). This energy is unlikely to be provided by the phosphate group. Not only that the needed −32 kcal/mol is without precedent but also it is in conflict with recent experiments. That is, Miller et al. (*11*, *37*) found only ∼15 kcal/mol (rather then 32 kcal/mol) for this contribution in the transition state analogue 6-hydroxyuridine 5′-phosphate (BMP). This contribution is only 7 kcal/mol larger than the overall substrate binding energy. This does not leave so much excess binding energy for the presumed GSD effect. This point is clarified in Figure 9, which compares the GSD and the TS stabilization mechanisms. The figure includes the actual energetics in water and in the protein as well as the assumed energetics for the case when the phosphoribosyl (which is designated by P^{2-}) is un-ionized but kept at the same orientation as that of the actual substrate (see below). In the GSD model we need the above-mentioned ∼32 kcal/mol stabilization upon moving from $[P^0S^-]_p$ to $[P^{2-}S^-]_p$. On the other hand, in the TS stabilization mechanism the contribution of P^{2-} to the binding free energy is only between 10 and 15 kcal/mol. It seems to us that the TS stabilization

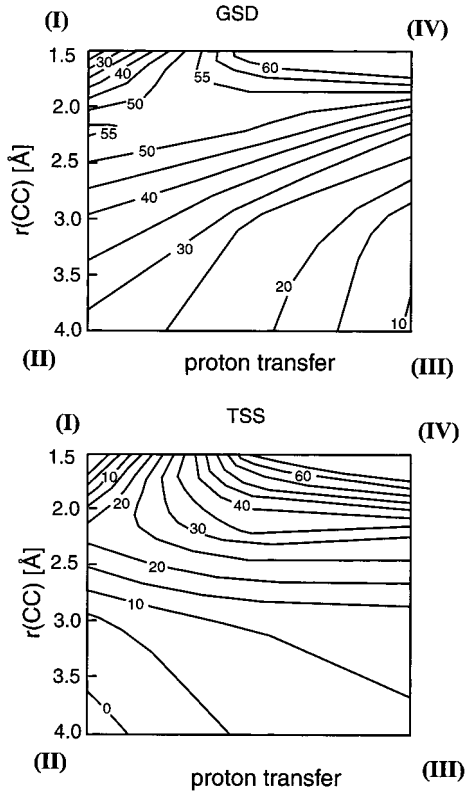

FIGURE 10: Qualitative examination of the effect of GSD and TS stabilization on the potential surface of the decarboxylation reaction. The upper figure was obtained by taking the solution surface and adding 20 kcal/mol to the reactant state and keeping the other corners unchanged while using linear interpolation for the change of other points on the surface. This reproduces the surface that we would have if the enzyme was working by a GSD mechanism. The lower surface was obtained by adding −10 and −30 kcal/mol, respectively, to corners I and II of the solution reaction and keeping the other corners unchanged, while using a linear interpolation for the change of other points on the surface. The resulting surface corresponds to the actual situation in ODCase. As seen from the figure if we had a GSD we should have consider the entire [S^-LH^+] system but such a consideration gives us the TS stabilization mechanism. The coordinate notations are the same as in Figure 7.

model looks much more reasonable than the GSD as much as the contribution of P^{2-} is concerned.

At this point, it is important to comment on the interesting issue of unstable ionized groups. As argued in this and in our previous works (*10*, *12*), it is unlikely to find a large GSD *at equilibrium* in systems that involve acids and bases with pK_a, which is not much different than 7. That is, if A denotes an acidic residue, the free energy for protonation of A^-_p in a protein site by a bulk proton H^+_p is given by the formula (*38*)

$$\Delta G(A^-_p + H^+ \rightarrow AH_p) = 2.3RT(\mathrm{pH} - \mathrm{p}K_a^p) = 2.3RT[(\mathrm{pH} - \mathrm{p}K_a^w) - (\mathrm{p}K_a^p - \mathrm{p}K_a^w)] = 2.3RT(\mathrm{pH} - \mathrm{p}K_a^w) - \Delta\Delta G^{w\rightarrow p}(A^-) \quad (1)$$

where pK_a^p and pK_a^w are the pK_as in water and in the protein, respectively, and $\Delta\Delta G^{w\rightarrow p}(A^-)$ is the free energy of the transfer of the ionized acid from water to the protein active site at standard conditions. [The positive values of $\Delta\Delta G^{w\rightarrow p}(A^-)$ characterize the magnitude of the destabilization of an ionized group in an protein interior.] In 1, we neglected the small

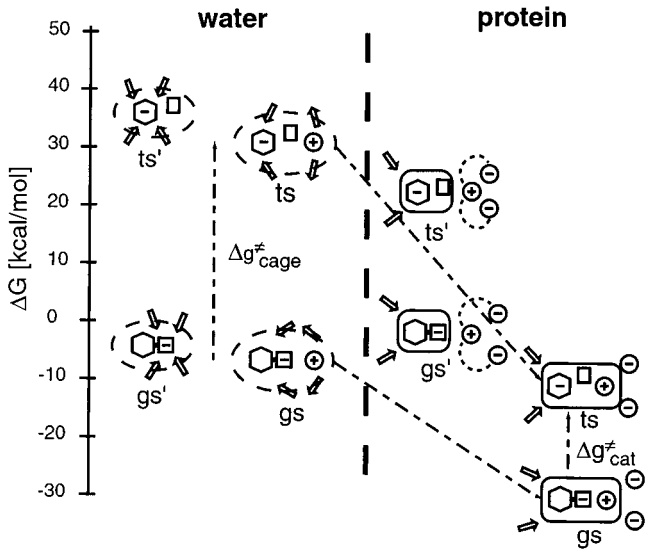

FIGURE 11: Energetics of the catalytic reaction of ODCase calculated for different alternative selections of region I. The figure represents a semiquantitative consensus from the Tables 1 and 2. The two diagrams separated by the vertical dashed line represent the energetics in water (left) and in the protein (right). The figure compares the energetics for the cases when region I includes [S^-] and [S^-LH^+]. These systems are designated by gs′ and gs (or ts′ and ts) respectively. The pyrimidine ring of the substrate and the carboxylate group (or CO_2) of the orotidine are described schematically as a hexagon and a square, respectively. The energy in the protein is taken relative to the corresponding energy in water. The energetics in water is taken relative to the corresponding neutral state at pH 7. The water dipoles of the molecules are described as arrows while Asp70 and Asp75b are described as negative charges. The energies of the different states present a qualitative estimate. As seen from the figure we obtain a modest GS stabilization and major TS stabilization with [S^-LH^+] in region I. With S^- in region I one obtains a small destabilization of the GS since the interaction between the ionized aspartic residues of the protein and $Lys72^+$ is not considered (only the *change* of this interaction is evaluated).

contribution of $\Delta\Delta G^{w\rightarrow p}(AH)$ to the proton-transfer free energy. Because for $\Delta G(A^-_p + H^+ \rightarrow AH_p) < 0$, the orotate becomes protonated (neutral), we obtain the upper limit for the equilibrium destabilization of A^- by an electrostatic repulsion as

$$\Delta\Delta G^{w\rightarrow p}(A^-) \leq 2.3RT(\mathrm{pH} - \mathrm{p}K_a^w) \quad (2)$$

Since orotic acid (SH) has a pK_a^w = 2.1 (*39*), the maximum equilibrium destabilization of orotate by the protein residues at pH 7 is about 6.7 kcal/mol. That is, if GSD is larger than 6.7 kcal/mol, then S^- will be protonated by a proton from the bulk water. Alternatively, protons can be transferred from other protein residues. It is instructive to point out, however, that our constraint on the magnitude of the GSD may be released in the exotic and new case of nonequilibrium conditions, where the reaction removes the unstable charge faster than the time needed for a penetration of an H_3O^+ ion. This can be the case if the barrier for proton transfer from solution to S^- is higher than the $\Delta g^{\ddagger}_{cat}$. However, this new nonequilibrium mechanism has clearly very little to do with all previously proposed GSD mechanisms that never considered nonequilibrium effects.

The most obvious problem with the GSD mechanism is the selection of the relevant reactive part (region I) of the GS and TS systems. That is, the actual reaction in the enzyme

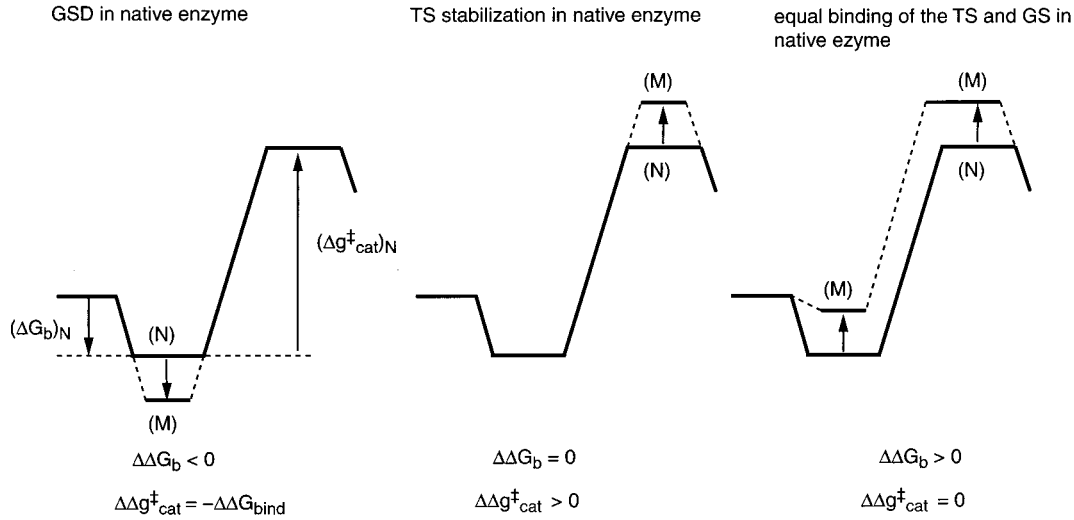

FIGURE 12: Illustrating the use of mutation experiments in discriminating between GSD and TS stabilization mechanisms. As is explained in the text, if the native enzyme (N) works by GSD then some mutants (M) should increase the stabilization of the GS. If the enzyme works by TS stabilization then some mutants should destabilize the TS. If the enzyme works by equal stabilization of the TS and the TS then some mutants will destabilize these states in an equal amount.

involves the substrate and Lys72 rather than only the substrate. Therefore, we should consider the $[S^-LH^+] \rightarrow [S'HL + CO_2]$ system rather than only the $[S^-] \rightarrow [S'H + CO_2]$ system. The extended definition of the reacting system yields an entirely different picture than that obtained while considering only its subset (Table 2). In this picture, the enzyme catalysis is clearly accomplished by TS stabilization rather than by GSD. Since some readers might question our selection of the $[S^-LH^+]$ as the reacting part we would like to re-emphasize that $LysH^+$ is a part of the reacting system since it transfers a proton to C6 during the reaction. Here, serine proteases (see, e.g., ref *40*) represent a classical example of a similar system, where the catalytic histidine residue serves as a proton acceptor (e.g., His 64 in subtilisin). Therefore, this residue is considered by all workers in the field as an integral part of the reacting system (see, for example, ref *41*). Still, it should be noted that the analogy between the role played by Lys and His residues in ODCase and serine proteases, respectively, may be questioned. This is because the activation barrier in our calculations corresponds to the motion from state I to state II in Figure 7, while the subsequent protonation step (II → III) is a downhill process. Therefore, one might argue that Lys72 should not be included in region I. However, this argument neglects the fact that with a GSD mechanism the enzyme reaction will become fully concerted and then the inclusion of $LysH^+$ in the reacting system becomes necessary (Figure 10). Thus, a careful mechanistic study should include the entire reacting system.

The origin of the TS stabilization is considered in Figures 2 and 11. In the GS the reacting system has a relatively small dipole moment since the carboxylate charge is neutralized by the nearby $LysH^+$ charge. In the TS this dipole increases significantly and so does its stabilization by its environment. This point is illustrated in Figure 11 where we show schematically that in the reference reaction we have to pay a very significant reorganization energy (λ) in order to bring the solvent dipoles to the configuration that stabilizes the ion pair TS. In the enzyme, in contrast, we have two relatively fixed negatively charged groups (Asp70 and Asp75b) that stabilize the $LysH^+$ part of the ion pair. These aspartate side chains are already preorganized in the active site in a configuration where they repel each other. Thus, the ODCase-catalyzed reaction does not involve as large reorganization energy as the reference solution reaction.

Naturally, the reader may wonder at this point why we obtain a different conceptual picture when the reacting system is limited to the substrate $[S^-]$ alone. The reason for such a dichotomy is also illustrated in Figure 11. That is, when we take $[S^-]$ as our reactant (region I), we miss the interaction between $LysH^+$ and the negatively charged Asp70 and Asp75b. This gives us a less stable "GS" rather than the actual GS, that is stabilized by the interaction between Lys72 and its surroundings. Note, however, that the calculation with $[S^-]$ in region I *does* include the *change* in the interaction of the two Asp residues and Lys72.

At this point, it is useful to consider the nature of the overall catalytic effect of ODCase. This effect is composed of a reduction of the difference between the free energy of the TS and GS (a reduction in $\Delta g^{\ddagger}_{cat}$) and from a reduction of $\Delta g^{\ddagger}$ (that corresponds to k_{cat}/K_M). The reduction of $\Delta g^{\ddagger}_{cat}$ is mainly due to the interaction between $[S^-LH^+]^{\ddagger}$ and the enzyme. As stated above, this contribution in largerly due to a preorganization effect. Also as stated in the previous section, it is possible that the lysine-assisted reference reaction has a barrier that is a few kilocalories per mol lower than that of the water assisted reaction. The rest of the catalytic effect is expressed in $\Delta g^{\ddagger}$ and not in $\Delta g^{\ddagger}_{cat}$. This is done by the well-understood effect of binding of the phosphoribosyl moiety, which stabilizes both the reactants and transition state (Figure 9). It is useful to point out in this respect the recent instructive experiment of Miller et al. (*37*), who measured the binding energies of the separate $[S^-]$ and the fragments as well as the rate for the separate $[S^-]$. This analysis has established that the phosphoribosyl leads to a very large transition-state stabilization (>11 kcal/mol). In our view, this effect is associated with bringing the $[S^-LH^+]$ system to its proper transition state orientation as well as preorganizing the complementary protein site (the Asp72 and Asp75B residues). Our previous study of ribonuclease (*46*, p. 10247) demonstrated and analyzed a similar

very large effect of the uracil moiety on the activation barrier for the hydrolysis of uridine methyl phosphate. More specifically, the presence of P^{2-} is crucial not only for binding of the [$P^{2-}S^{-}$] system but also for bringing it to the proper TS orientation and for forming the proper protein cavity around the TS.

As pointed out by one of us (*42*), it is possible to use mutation experiments to find out whether we have a GSD or TS stabilization. This is so since one can deduce from mutation experiments the change in the binding energy ($\Delta\Delta G_{bind}$) and in $\Delta g^{\ddagger}_{cat}$ ($\Delta\Delta g^{\ddagger}_{cat}$). If the mutated residue plays a crucial role in catalysis its removal will tell us how catalysis is achieved. If we have GSD then $\Delta\Delta G_{bind}$ should be negative (the native enzyme makes ΔG_{bind} more positive) and $\Delta\Delta g^{\ddagger}_{cat} = -\Delta\Delta G_{bind}$. If we have TS stabilization then $\Delta\Delta G_{bind} = 0$ and $\Delta\Delta g^{\ddagger}_{cat} > 0$ (see Figure 12). Mutations near the phosphate site (*37*) are consistent with TS stabilization but this is not conclusive since one really has to examine mutations near [S^{-}]. Such studies will be extremely instrumental in resolving the issue.

In summary, what we have here is an *electrostatic stress in the protein* (protein−protein interaction that includes the Asp70···Asp75b repulsion) rather than in the protein−substrate interaction. This is exactly our preorganization concept (*43*) where the enzyme folding energy is used to preorganize the active site polar environment of the GS in a configuration that is already complementary to the charge distribution of the TS. In this way the enzyme does not have to pay for reorganizations during the GS → TS process. Such an effect is fundamentally different than the GSD where the rate enhancement is presumed to be due to unfavorable enzyme−substrate interactions, rather than enzyme−enzyme interactions.

REFERENCES

1. Cohen, S. G., Vaidya, V. M., and Schultz, R. M. (1970) *Proc. Natl. Acad. Sci. U.S.A. 66*, 249−256.
2. Jencks, W. P. (1975) in *Advances in Enzymology and Related Areas of Molecular Biology* (Meister, A., Ed.) Vol. 43, J. Wiley & Sons, Inc., New York.
3. Dewar, M. J. S., and Storch, D. M. (1985) *Proc. Natl. Acad. Sci. U.S.A. 82*, 2225−2229.
4. Crosby, J., Stone, R., and Lienhard, G. E. (1970) *J. Am. Chem. Soc. 92*, 2891−2900.
5. Lee, J. K., and Houk, K. N. (1997) *Science 276*, 942−945.
6. Feng, W. Y., Austin, T. J., Chew, F., Gronert, S., and Wu, W. (2000) *Biochemistry 39*, 1778.
7. Appleby, T. C., Kinsland, C., Begley, T. P., and Ealick, S. E. (2000) *Proc. Natl. Acad. Sci. U.S.A. 97*, 2005−2010.
8. Wu, N., Mo, Y., Gao, J., and Pai, E. F. (2000) *Proc. Natl. Acad. Sci. U.S.A. 97*, 2017−2022.
9. Radzicka, A., and Wolfenden, R. (1995) *Science 267*, 90−93.
10. Warshel, A., and Florián, J. (1998) *Proc. Natl. Acad. Sci. U.S.A. 95*, 5950−5955.
11. Miller, B. G., Hassell, A. M., Wolfenden, R., Milburn, M. V., and Short, S. A. (2000) *Proc. Natl. Acad. Sci. U.S.A. 97*, 2011−2016.
12. Warshel, A. (1991) *Computer Modeling of Chemical Reactions in Enzymes and Solutions*, John Wiley & Sons, New York.
13. Warshel, A., Sussman, F., and King, G. (1986) *Biochemistry 25*, 8368.
14. Kollman, P. (1993) *Chem. Rev. 93*, 2395−2417.
15. Lee, F. S., Chu, Z. T., and Warshel, A. (1993) *J. Comput. Chem. 14*, 161.
16. Florián, J., and Warshel, A. (1997) *J. Phys. Chem. B 101*, 5583−5595.
17. Florián, J., and Warshel, A. (1999) *J. Phys. Chem. B 103*, 10282−10288.
18. Florián, J., and Warshel, A. (1998) *J. Phys. Chem. B 102*, 719−734.
19. Štrajbl, M., Florián, J., and Warshel, A. (2000) *J. Am. Chem. Soc. 122*, 5354−5366.
20. Frisch, M. J., Trucks, G. W., Schlegel, H. B., Gill, P. M. W., Johnson, B. G., Robb, M. A., Cheeseman, J. R., Keith, T., Petersson, G. A., Montgomery, J. A., Raghavachari, K., Al-Laham, M. A., Zakrzewski, V. G., Ortiz, J. V., Foresman, J. B., Cioslowski, J., Stefanov, B. B., Nanayakkara, A., Challacombe, M., Peng, C. Y., Ayala, P. Y., Chen, W., Wong, M. W., Andres, J. L., Replogle, E. S., Gomperts, R., Martin, R. L., Fox, D. J., Binkley, J. S., Defrees, D. J., Baker, J., Stewart, J. P., Head-Gordon, M., Gonzalez, C., and Pople, J. A. (1995) *Gaussian 94*, *Revision C.2*, Gaussian, Inc., Pittsburgh, PA.
21. Warshel, A., and Levitt, M. (1976) *J. Mol. Biol. 103*, 227−249.
22. Waszkowycz, B., Hillier, I. H., Gensmantel, N., and Payling, D. W. (1990) *J. Chem. Soc., Perkin Trans. 2*, 1259.
23. Bash, P. A., Field, M. J., Davenport, R. C., Petsko, G. A., Ringe, D., and Karplus, M. (1991) *Biochemistry 30*, 5826−5832.
24. Gao, J., and Xia, X. (1992) *Science 258*, 631−635.
25. Mulholland, A. J., Grant, G. H., and Richards, W. G. (1993) *Protein Eng. 6*, 133−147.
26. Bentzien, J., Muller, R. P., Florián, J., and Warshel, A. (1998) *J. Phys. Chem. B 102*, 2293−2301.
27. Åqvist, J., and Warshel, A. (1993) *Chem. Rev. 93*, 2523−2544.
28. Warshel, A., Sussman, F., and Hwang, J.-K. (1988) *J. Mol. Biol. 201*, 139−159.
29. Hwang, J.-K., King, G., Creighton, S., and Warshel, A. (1988) *J. Am. Chem. Soc. 110*, 5297.
30. Muller, R. P., and Warshel, A. (1995) *J. Phys. Chem. 99*, 17516−17524.
31. Lee, F. S., and Warshel, A. (1992) *J. Chem. Phys. 97*, 3100.
32. Sham, Y. Y., Chu, Z. T., and Warshel, A. (1997) *J. Phys. Chem. B 101*, 4458.
33. Sham, Y. Y., Muegge, I., and Warshel, A. (1998) *Biophys. J. 74*, 1744−1753.
34. Chu, Z. T., Villà, J., Schutz, C. V., and Warshel, A. (2000) Manuscript in preparation.
35. Warshel, A., Åqvist, J., and Creighton, S. (1989) *Proc. Natl. Acad. Sci. U.S.A. 86*, 5820.
36. Warshel, A., and Russell, S. T. (1984) *Q. Rev. Biol. 17*, 283.
37. Miller, B. G., Snider, M. J., Short, S. A., and Wolfenden, R. (2000) *Biochemistry 39*, 8113−8118.
38. Russell, S. T., and Warshel, A. (1985) *J. Mol. Biol. 185*, 389.
39. Serjeant, E. P., and Dempsey, B. (1979) in *Ionization Constants of Organic Acids in Aqueous Solution*, Pergamon Press, Oxford.
40. Warshel, A. N.-S., G., Sussman, F., and Hwang, J.-K. (1989) *Biochemistry 28*, 3629.
41. Daggett, V., Schroder, S., and Kollman, P. (1991) *J. Am. Chem. Soc. 113*, 8926−8935.
42. Warshel, A. (1998) *J. Biol. Chem. 273*, 27035−27038.
43. Warshel, A. (1978) *Proc. Natl. Acad. Sci. U.S.A. 75*, 5250.
44. Jencks, W. P. (1987) in *Catalysis in Chemistry and Enzymology* (Dover Ed.) Dover Publ., Inc.
45. Lide, D. R., Ed. (1991) *CRC Handbok of Chemistry and Physics* CRC Press, Boca Raton.
46. Glennon, T. M., and Warshel, A. (1998) *J. Am. Chem. Soc. 120*, 10234−10249.

BI000987H